ELSEVIER

Diamond and Related Materials 9 (2000) 825–830

DIAMOND AND RELATED MATERIALS

www.elsevier.com/locate/diamond

Elastic constants of ultrathin diamond-like carbon films

R. Pastorelli [a], A.C. Ferrari [b,*], M.G. Beghi [a], C.E. Bottani [a], J. Robertson [b]

[a] *INFM — Dipartimento di Ingegneria Nucleare, Politecnico di Milano, via Ponzio 34/3, I-20133 Milan, Italy*
[b] *Department of Engineering, University of Cambridge, Cambridge CB2 1PZ, UK*

Abstract

The determination of all the elastic constants of a supported film of thickness smaller than 1 μm is an unsolved problem. Various experimental procedures can be found in the literature, such as nano-indentation and laser spectroscopy methods based on the propagation of surface acoustic waves (SAWs), namely Surface Brillouin Scattering (SBS) and laser-induced SAWs. For the first time, the elastic constants of isotropic diamond-like films (ta-C and ta-C:H) have been determined by SBS from a modified Rayleigh wave and longitudinal guided mode. In SBS, the nano-mechanical response of the film is spontaneously probed by surface acoustic phonons scattering the light beam. A new fitting procedure gives a precise evaluation of the elastic constants even in the extremely difficult case of hard on soft structures. In contrast to nano-indentation, the Young's modulus, E, is determined directly. This provides a useful validation of the diverse approaches adopted to analyse nano-indentation data.

Keywords: Bonding; Brillouin scattering; Diamond-like carbon; Mechanical properties

1. Introduction

A diamond-like carbon (DLC) film is a random network of sp^2 sites, sp^3 sites and hydrogen sites; its mechanical properties depend mainly on the relative abundance of different kinds of carbon—carbon bonds: the film hardness and Young's modulus vary dramatically with sp^3 content, from the very low values of disordered graphite to values close to those of diamond. For this reason, the determination of the elastic constants of a DLC film is crucial for the characterisation of its mechanical behaviour with respect to its structure.

When the film thickness is considerably lower than 1 μm and the substrate is softer than the film, e.g. the DLC film is deposited on a silicon wafer, standard experimental procedures, as well as nano-indentation, are unable to determine the elastic constants of the DLC film: the difficulties of nano-indentation arise from the need to use an indentation depth less than 10% of the film thickness and its high sensitivity to the substrate when measuring hard films on a soft substrate. Nano-indentation actually measures the hardness, but the reduced Young's Modulus $E' = E/(1-\nu^2)$ can be derived by an Oliver–Pharr [1,2] analysis of the indentation curve, so that E itself can be found if a value for the Poisson's ratio, ν, is assumed. Nevertheless, nano-indentation has been widely employed to estimate the Young's modulus of DLC films, such as amorphous hydrogenated carbon (a-C:H) [1], tetrahedral amorphous carbon (ta-C) [2–4] and tetrahedral hydrogenated amorphous carbon (ta-C:H) [5]. The difficulties of this method are clear in that while the hardness values of ta-C are found to be between 60 GPa [2,4] and 90 GPa [3], the E' values vary more widely, from 400 GPa [2,4] to 1100 GPa [3].

More convenient approaches are based on laser spectroscopic methods related to the propagation properties of long wavelength acoustic phonons (surface acoustic waves, SAWs): surface Brillouin scattering (SBS), exploiting thermally activated SAWs [6], and laser-induced SAW techniques (LISAW) exploiting SAWs excited by laser irradiation [7]. Both SAW based methods offer the possibility of non-destructive measurements of the film elastic constants, but, though faster than SBS, LISAW is intrinsically less sensitive for film thickness below a fraction of a micrometre. In fact, the SAW penetration depth decreases with increasing frequency and SBS of visible light works in the 10–100 GHz range,

* Corresponding author. Tel.: +44-1223-332679; fax: +44-1223-332662.
E-mail address: acf26@eng.cam.ac.uk (A.C. Ferrari)

0925-9635/00/$ - see front matter
PII: S0925-9635(99)00245-9

while LISAW works in the 0.1–0.2 GHz range. Thus, SBS is the better technique to measure the Young's modulus, E, and the shear modulus, G, of thin supported films with a thickness of between several nanometres to hundreds of nanometres.

2. Experimental

In this work, SBS has been used to determine the elastic constants of two ta-C thin films (homogeneous and layered) and two ta-C:H, thin and very thin, films. The homogeneous ta-C film was deposited using an S-bend filtered cathodic vacuum arc (FCVA) [8,9] on a Si(100) wafer at room temperature at a mean ion energy of 100 eV and at a deposition rate of about 0.7 nm/s. The second layered ta-C thin film was deposited, with a single-bend FCVA system, always on the Si(100) wafer [8,9]. The ta-C:H films were deposited on Si(100) wafers from acetylene using an electron cyclotron wave resonance plasma source [10,11]. Both ta-C and ta-C:H films were preliminarily characterised with electron energy loss spectroscopy (EELS), X-ray reflectivity (XRR) [12], ellipsometry and profilometry to obtain the sp^3 content, density and thickness; the results are reported in Table 1; the internal stresses are also indicated. We assume that these amorphous films are elastically isotropic.

All these samples were investigated with SBS, with the same experimental set-up, to directly measure the propagation velocity of the SAW. As SAW velocities depend on physical quantities (i.e. density and elastic constants of the substrate and of the film) and on geometrical quantities (i.e. film thickness), the estimation of the film elastic constants is possible, solving an appropriate inverse problem (see below). This procedure is characteristic of all methods based on surface acoustic wave propagation.

SBS is the inelastic scattering of light by thermally excited SAWs via dynamical modulation of the dielectric function of the medium (the elasto-optic effect) and/or dynamic corrugation of the surface (the surface ripple). A Brillouin scattering measurement involves illuminating the specimen by a monochromatic laser light and analysing the spectrum of the scattered light (the spectra

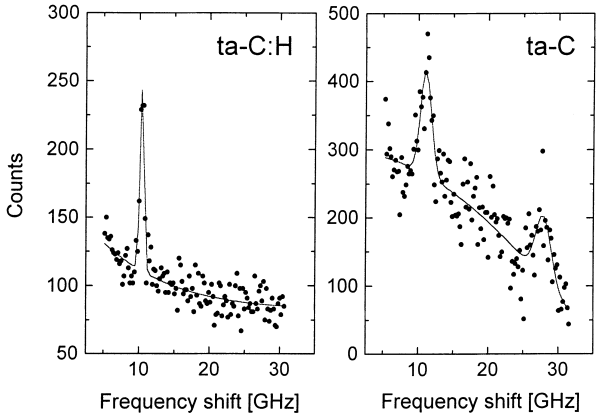

Fig. 1. Experimental Brillouin spectra of ta-C:H, 70 nm thickness, and layered ta-C. In ta-C:H, only the Rayleigh wave peak is visible, while in ta-C, also, a second peak, at ~28 GHz, associated with a pseudo-surface wave, can be seen. Both spectra are taken at 30°.

of the ta-C layered sample and of the ta-C:H, 70 nm thickness, are reported in Fig. 1): this is dominated by the elastically reflected light but also contains the components scattered by phonons: these last are shifted at frequency, ω. The scattering geometry selects the wavevector, $q_{\parallel}$, of the SAWs being probed; in backscattering configuration, adopted in this case, the scattering geometry is fully specified by the incidence angle θ: $q_{\parallel}=(4\pi/\lambda)\sin\theta$, λ being the laser wavelength. The wavelength of the phonons is $\lambda_{\parallel}=2\pi/q_{\parallel}=\lambda/(2\sin\theta)$; the spectral shift $(\omega/2\pi)$ directly supplies the phase velocities, v of specific SAWs: $v=\omega/q_{\parallel}$. For a film thickness below 500 nm, these phonons are dispersive: v varies with $q_{\parallel}$, the dispersion being stronger when the sound velocities of the film and the substrate are markedly different.

SBS spectra were recorded at room temperature in a backscattering configuration, with θ ranging from 30 to 70°; propagation was along the [100] direction on the (001) face of the Si substrate. The incident light is p-polarised; the scattered light is collected without polarisation analysis and analysed by a tandem 3+3 pass high contrast interferometer of the Sandercock type with a finesse of about 100. The light source was an argon ion laser operating at $\lambda=514.5$ nm. The incident power on the specimen was around 130 mW, focused into a spot of the order of 10^3 μm^2; structural stability under

Table 1
Sample properties

Specimen		sp^3 content (%)	Plasmon energy (eV)	Density (g/cm^3)	Thickness (nm)	Internal stress (GPa)	Hydrogen content (%)
ta-C	Homog.	88	31.8	3.26	76	10	
ta-C	Surf. lay.			2.70	7		
(layered)	Bulk.lay.	85 (av.)	31.4 (av.)	3.24	63.5		
ta-C:H	Homog.	70	28.4	2.35	70	6	~30
ta-C:H	Homog	70	28.4	2.35	43	8.4	~30

irradiation was ascertained. The experimental SAWs dispersion curves are shown in Fig. 2.

3. Results

The solution of the inverse problem, i.e. the derivation of the elastic constants from measured SAW velocities, uses the solution of the direct problem, i.e. the computation of SAW velocities from given elastic constants. The SAW velocities, depending on the film thickness and density and elastic constants, and on the substrate elastic constants and density, can be computed by Green's function methods [6].

The substrate can be anisotropic, leading to a dependence of the dispersion relation on the wavevector direction, while the isotropy of the film means that its elastic properties are fully defined by only two independent quantities. The two independent quantities are typically taken as the two elements C_{11} and C_{44} of the elastic tensor, or any two among the four quantities E (Young's modulus), G (shear modulus; for isotropic film $G=C_{44}$), v (Poisson's ratio) and B (bulk modulus); the relations among all of them are well known.

The elastic properties of the substrate are known (for Si substrate $C_{11}=166$ GPa, $C_{12}=63.9$ GPa, $C_{44}=79.6$ GPa) as well as its density ($\rho=2.33$ g/cm^3) and the propagation direction of the acoustic wave. The film thickness and density were obtained by XRR and EELS, so the acoustic velocities remain functions of the unknown elastic constants of the film. The elastic properties can be specified by any pair among the elastic constants mentioned above; adopting (E, G) the velocities v_e^i (E, G) are computed at each $q_\parallel$ (i.e. at each incidence angle) in a rectangular mesh of values of the elastic constants E and G, encompassing a physically significant interval. For each film, the couple $(E, G)_{film}$ is derived by fitting the calculated velocities, v_c, to the experimental velocities, v_e, to minimise the residual R:

$$R=\sum\left(\frac{v_e^i(E,G)-v_e^i}{\sigma_e^i}\right)^2, \quad (1)$$

where σ_e^i (of the order of 30 m/s) are the contributions to the variance of the corresponding v_e^i due to the statistical errors intrinsic to the measurement.

The elastic moduli that minimise R are the most probable solution of the inverse problem; the region corresponding to any fixed confidence level is also recognisable. It must be remembered that the elastic properties of the film are defined by a point in the (E, G) plane or equivalently, in the (E, v) or (B, G) or similar planes. The elastic constants must satisfy thermodynamic stability requirements, so any of these planes includes regions that are physically meaningful and regions that are not. Any region in the (E, G) plane can be mapped in a corresponding region in the (E, v) or (B, G) or other planes. The transformations among these planes are not trivial, and the shapes of the transformed regions can be quite different from each other. This is particularly relevant for the regions corresponding to given confidence levels: it easily happens that in one such plane, the region is approximately elliptical, giving a rather defined estimate of both the independent parameters, while in another plane, it becomes very elongated along one axis or crushed on the thermodynamic limits, meaning an almost complete indetermination of that parameter [13]. In general, E and G constitute the best couple for the fitting procedure. As far as the bulk modulus, B, is concerned, its accessibility by means of SBS depends strictly on the specific surface phonon spectrum and its visibility in terms of scattering cross-section.

Generally, the surface projected spectrum of long-wavelength acoustic phonons of a homogeneous semi-infinite body for a given surface phonon wavevector is the combination of a *discrete* (low-frequency) set and a *continuous* (high frequency) set. In the discrete part, peaks corresponding to true surface waves (surface bounded modes) show up: *true surface resonances*. In the discrete part, *the Rayleigh wave* is found. In the continuous part, peaks corresponding to wave-packets of bulk waves with a partial surface localization (pseudo-surface waves) can exist: *quasi-resonances*. Among the quasi-resonances, the sole relevant excitation of a isotropic surface is the *High Frequency Pseudo Surface Wave* (HFPSW) or *Longitudinal Resonance* (LR) [14]. This wave propagates parallel to the surface with the same speed as longitudinal bulk phonons. Its visibility

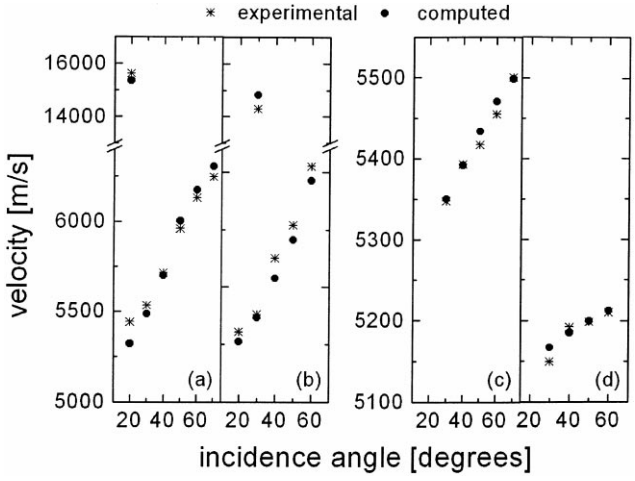

Fig. 2. Dispersion curves of surface waves for the investigated samples: (a) homogeneous ta-C; (b) layered ta-C; (c) ta-C:H, 70 nm thickness; (d) ta-C:H, 43 nm thickness. The lower branch is the modified Rayleigh wave; the upper, in (a) and (b), consisting of only one point (due to cross-section problems), is the longitudinal guided mode.

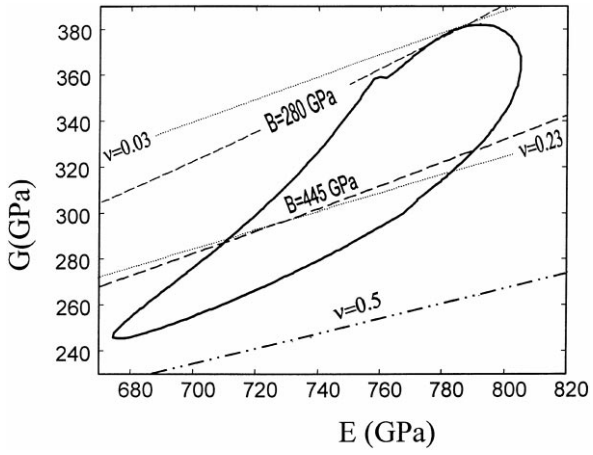

Fig. 3. E, G confidence plot for a homogeneous ta-C film. The solid contour line defines the 95% confidence region. The dashed lines and dotted lines define the corresponding intervals for B and v. The zone above the lowest dashed dotted line is the region of thermodynamic stability.

in a SBS experiment depends on the strength of the elasto-optic coupling of the medium, as the LR is polarised along its propagation direction and cannot be seen by the surface ripple mechanism.

In the case of a supported film, the LR modifies into the *Longitudinal Guided Mode* (LGM), partially confined in the film, if the sound speed of the film is lower than the sound speed of the substrate. If sound is faster in the film, the partial localisation is always near the surface but less in the film, and *Modified Longitudinal Resonance* (MLR) would be a more appropriate name for this excitation. As the longitudinal sound speed is $v_L=\sqrt{(B+4G/3)/\rho}$, the LR (or its modified version) is also particularly sensitive to the B value.

Both ta-C samples show two branches of the SAWs dispersion curve, the modified Rayleigh wave (MRW) and the pseudo surface mode, the longitudinal guided mode, as firstly reported in [15]; both ta-C:H samples show the only branch of the SAW dispersion relation, the MRW. The MRW allows a precise determination of E and G intervals, whilst it is less sensitive to the bulk modulus, B, and the Poisson's ratio, v. However, the LGM provides more information related to the bulk modulus.

Data analysis for homogeneous ta-C film shows the 95% confidence region corresponding to a bulk modulus lower than diamond (445 GPa) for the (E, G) pair, represented in Fig. 3; the corresponding values are 710–805 GPa for E and 290–385 GPa for G. This region selects wider intervals for the bulk modulus, Poisson's ratio pair (B, v). This gives $B=280$–445 GPa and $v=0.03$–0.23. The average $E=757.5$ GPa and $G=337.5$ GPa give $B=334$ GPa and $v=0.12$, as summarised in Table 2.

The ta-C film from single-bend FCVA is not homogeneous. It was modelled as two homogeneous layers: a *external layer* 7 nm thick, with a density of 2.7 g/cm^3 and a *internal layer* 63.5 nm thick, with density of 3.24 g/cm^3[12]. Given this layered nature, the corresponding computed velocities depend on the (E, G) couple both of the external film layer and of the internal film layer. Given the few experimental points compared to the number of unknown parameters, the above data analysis procedure was not strictly applied. However, the residual, R, shows a weak dependence of the modified Rayleigh wave on $(E, G)_{ext}$ and a strong dependence on E_{int}, allowing a reliable determination of E_{int}. This was adopted as a first guess to fit G_{int} and $(E, G)_{ext}$ using both MRW and LGM. The non-removable difference between experimental and computed velocity for the LGM (see Fig. 2) is to be connected to the model adopted for the film schematisation: two homogeneous layers, even though the external layer of the real film probably has a density gradient. The final values are $E_{int}=750$–790 GPa, $G_{int}=300$–395 GPa, $E_{ext}=200$–300 GPa, while $G_{ext}=70$–150 GPa. This procedure shows that the Young's modulus of a 7 nm thick overlayer can be obtained by SBS, provided an accurate data treatment is used. Such ultrathin carbon layers, which are used for coating magnetic storage disks, cannot be probed by conventional nano-indentation.

For the ta-C:H film of 70 nm thickness, the 95% confidence region corresponding to a bulk modulus lower than diamond covers the range $E=291$–304 GPa and $G=105$–116 GPa. This corresponds to a wider range of bulk modulus and Poisson's ratio values: $B=248$–445 GPa, the upper bound being the bulk modulus of diamond (445 GPa), $v=0.3$–0.39. This means that B is essentially indeterminate, in that the computed v_c^i (E,G) are sensitive to E and G and almost insensitive to

Table 2
Elastic constants of our films, compared to the isotropic (Voigt–Reuss–Hill) average for diamond and for the 100% sp^3 random network simulation of WWW-ta-C [19]

	Ta-C:H	ta-C	ta-C^{surf}	WWW-ta-C	Diamond
E (GPa)	300^{+4}_{-9}	757.5 ± 47.5	200–300	822.9	1144.6
G (GPa)	115^{+1}_{-10}	337.5 ± 47.5	70–150	366	534.3
B (GPa)	248^{+197}_{-0}	334^{+111}_{-54}	>67	365	444.8
v	$0.3^{+0.09}_{-0}$	$0.12^{+0.11}_{-0.09}$	0–0.43	0.124	0.07

B. We note that ta-C:H has a density of 66% of diamond and 30 at.% hydrogen, and we can assume the minimum computed B of 248 GPa as the bulk modulus of ta-C:H, by scaling from the B of diamond. This sets the Poisson's ratio to 0.3.

This is confirmed by the indication coming from the residual minimisation of the other ta-C:H film (43 nm thick), for which the most probable values for the (E,G) couple are, respectively, 260 and 98 GPa; correspondingly, we found $B=250$ GPa and $v=0.33$, in agreement with the above predictions.

4. Discussion

We now compare our results to previous studies. Our E values confirm the values of Schneider et al. [7,16] and Morath et al. [17] on films of a similar density. This is because SAW-based methods are highly sensitive to Young's modulus [13], so they yield good values even using less film-probing methods, such as laser-induced SAW. The SAWs are less sensitive to the Poisson's ratio, thus explaining our lower accuracy for v and why an assumption of v is necessary in laser-induced SAW. However, the nano-indentation is seen to grossly underestimate E for ta-C, giving values of 400–500 GPa [2,4]. Knapp et al. [3,18] proposed a finite-element model to overcome the limitations of the Oliver–Pharr [2,4] analysis of the indentation curve, but this model now seems to overestimate E at 1020–1100 GPa.

Our data indicate that the Young's modulus of ta-C:H, 300 GPa, is much lower than in ta-C, in this case similar to that found previously in thick ta-C:H films by nano-indentation [5]. Clearly, the hydrogen content of ta-C:H has strongly reduced its network rigidity. Comparing our E data for ta-C with those of Schultrich et al. [16], we verified, for a pure carbon network, the constraint-counting theory of the elastic properties of random covalent networks [15]. The extrapolated E for a coordination of 4 was $\sim$800 GPa [15]. This value is considerably less than the isotropic average E of diamond, 1144 GPa. It is closer to the modulus found in a molecular dynamics simulation of a 100% sp^3 random network of a-C [19] (Table 2). This suggests that random networks may be softer than the isotropic averages of the corresponding crystal. A similar softening of elastic constants is seen in a-Si [20].

Table 2 also compares the Poisson's ratios of ta-C and ta-C:H and the isotropic average of diamond. Diamond has a uniquely low v for covalent materials, as does ta-C. This is presumably due to a high bond-angle rigidity of carbon's sp^3 bonds. However, v of a-C:H was previously found to be quite high, 0.3–0.4 [1]. Our more precise determination finds that ta-C:H has a similar v of 0.3 or over. This suggests the C—H bonding in ta-C:H and a-C:H gives both the larger Poisson's ratio.

5. Conclusions

We have shown that surface Brillouin scattering remains the best technique by which to measure the elastic constants of thin and, in particular, very thin (<10 nm) supported films. Even in the case of fast films on slow substrates, typical of hard DLC films, an appropriate data analysis provides a precise estimate of Young's modulus and shear modulus. When two different phonon branches, namely the modified Rayleigh wave and the longitudinal guided mode, are measurable, the bulk modulus too becomes directly accessible.

Acknowledgements

M.G.B., C.E.B. and R.P. acknowledge financial support from 'Progetto Finalizzato Materiali Speciali per Tecnologie Avanzate II' of Consiglio Nazionale delle Ricerche. A.C.F. acknowledges funding by a European Community TMR Marie Curie Fellowship.

References

[1] X. Jiang, K. Reichelt, B. Stritzker, J. Appl. Phys. 68 (1990) 1018.
[2] G.M. Pharr, D.L. Callahan, S.D. McAdams, T.Y. Tsui, S. Anders, J.W. Ager, I.G. Brown, C.S. Bhatia, S.R.P. Silva, J. Robertson, Appl. Phys. Lett. 68 (1996) 779.
[3] T.A. Friedman, J.P. Sullivan, J.A. Knapp, D.R. Tallant, D.M. Follstaedt, D.L. Medlin, P.B. Mirkarimi, Appl. Phys. Lett. 71 (1997) 3820.
[4] S. Xu, D. Flynn, B.K. Tay, S. Prawer, K.W. Nugent, S.R.P. Silva, Y. Lifshitz, W.I. Milne, Phil. Mag. B 76 (1997) 351.
[5] M. Weiler, S. Sattel, T. Giessen, K. Jung, H. Ehrhardt, J. Robertson, Phys. Rev. B 53 (1996) 1594.
[6] M.G. Beghi, C.E. Bottani, P.M. Ossi, T. Lafford, B.K. Tanner, J. Appl. Phys. 81 (1997) 672.
[7] D. Schneider, C.F. Meyer, H. Mai, B. Schoeneich, H. Ziegele, H.J. Scheibe, Y. Lifshitz, Diamond Relat. Mater. 7 (1998) 973.
[8] P.J. Fallon, V.S. Veerasamy, C.A. Davis, J. Robertson, G.A.J. Amaratunga, W.I. Milne, Phys. Rev. B 48 (1993) 4777.
[9] M.C. Polo, J.L. Andujar, J. Robertson, W.I. Milne, Diamond Relat. Mater. 9 (2000) 663.
[10] M. Weiler, K. Lang, E. Li, J. Robertson, Appl. Phys. Lett. 72 (1998) 1314.
[11] N.A. Morrison, S.E. Rodil, A.C. Ferrari, J. Robertson, W.I. Milne, Thin Solid Films 337 (1999) 71.
[12] A. Libassi, A.C. Ferrari, V. Stolojan, B.K. Tanner, J. Robertson, L.M. Brown, Diamond Relat. Mater. 9 (2000) 771.
[13] S. Tarantola, R. Pastorelli, M.G. Beghi, C.E. Bottani, in: Mathematical and Statistical Methods for Sensitivity Analysis, A. Saltelli, K. Chan, M. Scotts (Eds.), Probability and Statistics Series, John Wiley and Sons, New York, 2000.
[14] F. Nizzoli, J.R. Sandercock, in: Surface Brillouin Scattering from Phonons, G.K. Norton, A.A. Maradudin (Eds.), Dynamical

Properties of Solids Vol. 6 , North Holland, Amsterdam, 1990, p. 281.
[15] A.C. Ferrari, J. Robertson, M.G. Beghi, C.E. Bottani, R. Ferulano, R. Pastorelli, Appl. Phys. Lett. 75 (1999) 1893.
[16] B. Schultrich, H.J. Scheibe, D. Dresher, H. Ziegle, Surf. Coat. Technol. 98 (1998) 1097.
[17] C.J. Morath, H.J. Maris, J.J. Cuomo, D.L. Pappas, A. Grill, V.V. Patel, J.P. Doyle, K.L. Saenger, J. Appl. Phys. 76 (1994) 2636.
[18] J.A. Knapp, D.M. Follstaedt, S.M. Myers, J.C. Barbour, T.A. Friedmann, J. Appl. Phys. 85 (1999) 1460.
[19] P.C. Kelires, Phys. Rev. Lett. 73 (1994) 2460.
[20] S.I. Tan, B.S. Berry, B.L. Crowder, Appl. Phys. Lett. 20 (1972) 88.